Article

Not peer-reviewed version

A one-dimensional semaglutide-GLP-1R-based mini static GIBAC

Wei Li *

Posted Date: 14 June 2024

doi: 10.20944/preprints202406.0953.v1

Keywords: GIBAC; Intermolecular binding affinity (Kd); Structural biophysics; Synthetic data; Drug discovery \& design;

Article

A one-dimensional semaglutide-GLP-1R-based mini static GIBAC

Wei Li *

Posted Date: 14 June 2024

doi: 10.20944/preprints202406.0953.v1

Keywords: GIBAC; Intermolecular binding affinity (Kd); Structural biophysics; Synthetic data; Drug discovery \& design;

 doi:10.20944/preprints202406.0953.v1

Article

A One-Dimensional Semaglutide-GLP-1R-Based Mini Static GIBAC

Wei Li

Contrebola Institute of Computational Interstructural Biophysics, No. 88, Fuxing East Road, Nantong City 226000, Jiangsu Province, People's Republic of China; wli148@aucklanduni.ac.nz

Abstract: Drug-target binding is an essential parameter in drug discovery and design to ensure drug efficacy and specificity. In 2022, the concept of a general intermolecular binding affinity calculator (GIBAC) was for the first time coined: $K_d = f(molecules, envPara)$. Technically, GIBAC represents a set of in silico approaches for structural and biophysical data generation towards a paradigm shift in precise drug discovery and design, providing a comprehensive framework for intermolecular binding affinity calculation with adequate accuracy, precision and efficiency. For the first time, this study reports a prototype of GIBAC (semaGIBAC), i.e., a one-dimensional semaglutide-GLP-1R-based mini static GIBAC, based on an experimental complex structure of semaglutide and GLP-1R. Semaglutide is a potent GLP-1 receptor agonist used to treat type 2 diabetes mellitus by regulating blood glucose levels and promoting weight loss. In 2021, a structural modification involving a Val27-Arg28 exchange was manually introduced to enhance semaglutide-GLP-1R binding affinity. This study employs a comprehensive structural and biophysical analysis aimed at thoroughly exploring the sequence space of semaglutide-GLP-1R to design analogues with improved binding affinity, leading to the identification of a promising semaglutide analogue, which binds to GLP-1R with an affinity that is more than two orders of magnitude (113.3 times) higher than native semaglutide. To sum up, this article puts forward a promising structural biophysical approach for developing GLP-1 receptor agonists with enhanced efficacy, and with a GIBAC prototype (semaGIBAC), this article argues again that the time is now ripe for the construction of a real GIBAC to be listed on the agenda of the drug discovery and design community.

Keywords: GIBAC; intermolecular binding affinity (K_d); structural biophysics; synthetic data; drug discovery & design;

1. Introduction

1.1. Intermolecular Binding Affinity in Drug Discovery and Design

Intermolecular interactions are the fabrics underlying almost all processes in living organisms [1–8], where two cornerstone concepts, intermolecular binding affinity (K_d) and free binding energy (ΔG), have long been established to physically describe the strengths of biomolecular interactions [9–15]. Intermolecular binding affinity, e.g., drug-target binding affinity (K_d and ΔG), is an essential parameter in drug discovery and design to ensure efficacy and specificity [6,11,16–21]. First, high binding affinity typically correlates with increased efficacy, i.e., the drug can effectively modulate the target's activity at lower concentrations [22–28]. Second, a structural biophysical understanding of the intermolecular binding affinity helps in optimizing the potency and selectivity of drug candidates, reducing off-target effects and adverse reactions [29–34].

In August of 2022, therefore, the concept of a general intermolecular binding affinity calculator (GIBAC) was for the first time coined, proposed and defined as $K_d = f(molecules, envPara)$ [35]. Last October, GIBAC was for the first time updated, including its inception, definition, construction, practical applications, technical challenges and limitations and future directions [36]. With the conceptual and practical framework of GIBAC in place [36], this article puts forward a hypothesis

 doi:10.20944/preprints202406.0953.v1

that a real GIBAC technically makes sense and is feasible, and aims to test this hypothesis through the construction of a prototype of a real GIBAC [4,35,36].

1.2. Building a GIBAC Prototype with Semaglutide as an Example

In principle, any biomolecule inside Protein Data Bank [37–41] is fit to be used to build a prototype of a real GIBAC [4,35,36]. Here, this article chooses semaglutide due to the availability of abundant experimental data and clinical relevance of semaglutide [42,43]. First, semaglutide is a synthetic long-acting analogue of glucagon-like peptide-1 (GLP-1), which has garnered significant attention for its efficacy in treating type 2 diabetes and obesity [44,45]. Structurally, its direct binding and interaction with the GLP-1 receptor involves intricate mechanisms, where the complex structure has already been experimentally determined with Cryo-EM or X-ray diffraction (Tables 1 and 2, Figure 1) [42]. From a chemical structure point of view, semaglutide is a peptide-based molecule, including a peptide backbone consisting of 31 amino acids (a modified version of human GLP-1, 7-37), a substitution of alanine with 2-aminoisobutyric acid (an unnatural amino acid [46–48]) at position 8 to resist enzyme degradation, and an addition of a C-18 fatty acid chain attached via a spacer (γ-Glu-2x-OEG) at lysine 26 for stronger albumin binding [29,49].

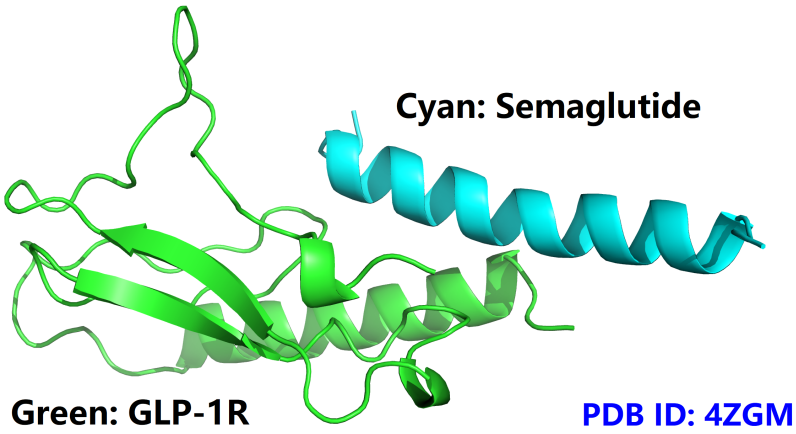

Figure 1. Crystal structure of semaglutide backbone in complex with the GLP-1 receptor extracellular domain.

In short, semaglutide is neither small molecule compound, nor monoclonal antibody, nor ADC/PDC, nor an entirely peptide-based drug, making it a reasonable choice as an example for the construction of a GIBAC prototype, i.e., a one-dimensional semaglutide-GLP-1R-based mini static GIBAC, abbreviated below as semaGIBAC and described in Equation 1:

$$K_{\mathrm{d}} = f(ABcomplex, seqA, seqB, center, n, r, T, mList) \tag{1}$$

where $ABcomplex$ represents the experimental complex structure of $molA$ and $molB$, $seqA$ and $seqB$ represent the amino acid sequences of $molA$ and $molB$, respectively, $center = molA$, or $molB$ or both, n represents the number of missense mutations introduced into the sequence of $center$, r represents the number of structural models built by Modeller [50], T represents temperature [51–54], and $mList$ represents the site-specific mutations introduced into the backbone of semaglutide (PDB entry 4ZGM [42], Table 2).

Table 1. Experimentally determined semaglutide-related structures in Protein Data Bank (QUERY: Polymer Entity Description = "Semaglutide").

PDB ID	Structure Title
7KI0	Semaglutide-bound Glucagon-Like Peptide-1 (GLP-1) Receptor in Complex with Gs protein

 doi:10.20944/preprints202406.0953.v1

Table 2. Experimentally determined semaglutide-related structures in the Protein Data Bank (QUERY: Full Text = "Semaglutide").

PDB ID	Structure Title (release date from newest to oldest)
7KI0	Semaglutide-bound Glucagon-Like Peptide-1 (GLP-1) Receptor in Complex with Gs protein
7KI1	Taspoglutide-bound Glucagon-Like Peptide-1 (GLP-1) Receptor in Complex with Gs Protein
4ZGM	Crystal structure of semaglutide backbone in complex with the GLP-1 receptor extracellular domain

2. Materials and Methods

To build a prototype of a real GIBAC, as mentioned above, this article chooses semaglutide due partly to the availability of abundant experimental data of semaglutide [42,43]. Among the three experimental complex structures of semaglutide and GLP-1R (Table 2), there is only one experimental structure (X-ray diffraction) of the semaglutide backbone in complex with the extracellular domain of GLP-1R (Figure 1, PDB ID: 4ZGM [42]).

According to PDB entry 4ZGM [42] (Table 2), the sequences of the two chains of semaglutide backbone and GLP-1R are listed in italics in fasta format as below,

>4ZGM_1_Chain A (Figure 1)

RPQGATVSLWETVQKWREYRRQCQRSLTEDPPPATDLFCNRTFDEYACWPDGEPGSFVNVSC PWYLPWASSVPQGHVYRFCTAEGLWLQKDNSSLPWRDLSECEESKRGERSSPEEQLLFLY

>4ZGM_2_Chain B_a modified version of human GLP-1 (7-37) (Figure 1)

HAEGTFTSDVSSYLEGQAAKEFIAWLVRGRG

In 2021, a Val27-Arg28 exchange (Table 3) was for the first time introduced into the backbone of semaglutide to strengthen the semaglutide-GLP-1R binding affinity to $\sim$ one-third of the K_d between native semaglutide and GLP-1R [6,55,56].

Table 3. Strengthening semaglutide-GLP-1R binding affinity via a Val27-Arg28 exchange in the peptide backbone of semaglutide.

PDB file	Protein-Protein Complex	Δ G (kcal/mol)	Kd (M) at 37 °C	Fold
4ZGM [42]	semaglutide-GLP-1R [42]	-7.8	3.4×10^{-6}	1
sema.pdb [6]	Val27-Arg28 exchange [6]	-8.4	1.1×10^{-6}	3.09

First, with PDB entry 4ZGM [42] (Table 2) in place, Modeller [50] was employed to build 10000 structural models with 100% homology to PDB ID: 4ZGM [42], the binding affinities between semaglutide and GLP-1R were calculated using Prodigy [57,58] 10000 times [59]. Second, with PDB entry 4ZGM [42] (Table 2) in place as an initial input, the process of the construction of a prototype GIBAC (semaGIBAC, Equation 1) subsequently consists of an automated in silico generation of synthetic structural and K_d data, as illustrated in Figure 2 and described previously in detail [60]. Briefly, Modeller [50] was employed to build a total of 11200 ($\frac{28!}{1!(27)!} \times 20^1 \times 20$) homology structural models with 95.42% (27/28) homology to PDB ID: 4ZGM [42]. Afterwards, the binding affinities between semaglutide analogues and GLP-1R were calculated using Prodigy [57,58] for 11200 times [59].

 doi:10.20944/preprints202406.0953.v1

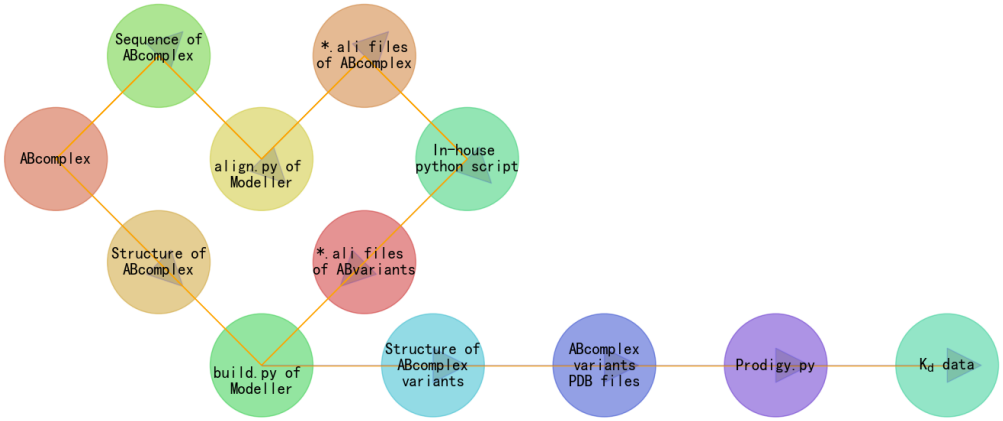

Figure 2. Automated in silico generation of synthetic structural and K_d data.

3. Results

With PDB entry 4ZGM [42] (Table 2) as an initial input and an automated in silico generation of synthetic structural and K_d data [60], this article for the first time puts forward a prototype GIBAC, i.e., semaGIBAC, for which everything is included in **Table S1** of supplementary file semaGIBAC.pdf:

$$K_d = f(SGcomplex, seqS, seqG, sema, n, r, T, mList) \quad (2)$$

where $SGcomplex$ represents PDB entry 4ZGM [42] (Table 2), $seqS$ and $seqG$ represent sequences of semaglutide backbone ($molA$) and GLP-1R ($molB$), respectively, $center = semaglutide$, n =1, r =20 [50], T = 37°C. Of further note, here, $center = semaglutide$ indicates that site-specific missense mutation is introduced only into the backbone of semaglutide, but not into GLP-1R (PDB entry 4ZGM [42], Table 2), making semaGIBAC a semaglutide-centered GIBAC prototype [35,36].

In Figure 3 and Table 4, for PDB entry 4ZGM [42] (Table 2), most of the K_d values are located between 2.5 × 10^{-6} M and 4.0 × 10^{-6} M, with an average at 3.278 × 10^{-6} M, which is rather close to the one K_d (3.4 × 10^{-6} M) as reported previously [6,59]. In Figure 3 and Table 4, for the 11200 homology structural models (semaGIBAC), most of the K_d values are located between 2.0 × 10^{-6} M and 4.0 × 10^{-6} M, with minimum and maximum values at 4.1 × 10^{-7} M and 9.4 × 10^{-6} M, respectively. From Figure 3 and Table 4, it can be seen that the the range of the K_d values gets wider and wider as n (Equations 1 and 2) increases from zero to one and to two.

Table 4. Statistics of the intermolecular binding affinities of PDB entry 4ZGM (Table 2), semaGIBAC and an incomplete two-dimensional semaGIBAC.

Model	Repeat	Mean	Std	Min	Max
4ZGM [42]	10000	3.278E-06	7.800E-07	1.100E-06	8.900E-06
semaGIBAC	11200	3.134E-06	1.091E-06	4.100E-07	9.400E-06
2D semaGIBAC	154055	3.402E-06	1.400E-06	1.400E-07	1.500E-05

 doi:10.20944/preprints202406.0953.v1

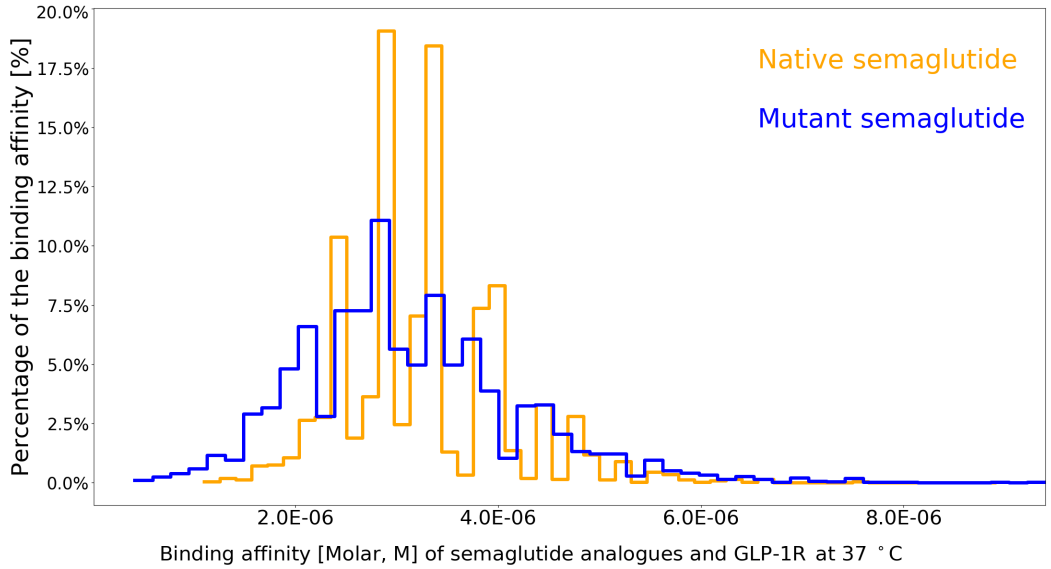

Figure 3. Distribution of the binding affinities between native semaglutide and GLP-1R (10000 structural models) and between semaglutide mutants/analogues (with one missense mutation) and GLP-1R (11200 structural models).

As described above, the semaGIBAC here is built to be a one-dimensional semaglutide-GLP-1R-based semaglutide-centered mini static GIBAC [35,36]:

1. semaGIBAC is a one-dimensional GIBAC, i.e., $n = 1$ (Equations 1 and 2).
2. semaGIBAC is a semaglutide-GLP-1R-based GIBAC, i.e., PDB entry 4ZGM [42] (Table 2) is the initial input before the construction of semaGIBAC.
3. semaGIBAC is a semaglutide-centered GIBAC, i.e., missense mutation is introduced only into the backbone of semaglutide (PDB entry 4ZGM [42]).
4. semaGIBAC is a mini GIBAC, i.e., semaGIBAC is able to calculate intermolecular K_d only between GLP-1R and semaglutide (analogues) with one mutation.
5. semaGIBAC is a static GIBAC, i.e., semaGIBAC does take conformational dynamics [61,62] into account.

Last October, GIBAC was for the first time updated, including its inception, definition, construction, practical applications, technical challenges and limitations and future directions, including in particular a set of criteria as listed below [35,36]:

1. a real GIBAC [4,35,36] needs to take site-specific mutations into account;
2. structural biophysics is inextricably linked to and at the core of a real GIBAC [4,35,36], e.g., accurate structural information is necessary [63–65];
3. for a real GIBAC [4,35,36], a variety of intermolecular K_d-relevant factors need to be taken into account, such as temperature, pH [66–68], side chain pKa of protein [51,58,69–72], ionic strength and buffer conditions [54,58,73–76], etc;
4. a real GIBAC [4,35,36] requires an accurate general forcefield for all atoms [46];
5. a real GIBAC [4,35,36] requires a universal linear string/graph-based notation system for all molecular types and drug modalities [61,77];
6. a real GIBAC is able to be used the other way around as a search engine for drug discovery & design [4,35,36].

Nonetheless, this article puts forward just only a prototype (i.e., semaGIBAC), instead of a real GIBAC. Specifically,

1. semaGIBAC does take one missense mutation into account;

 doi:10.20944/preprints202406.0953.v1

2. structural biophysics is at the core of semaGIBAC;
3. semaGIBAC takes only some K_d-relevant factors into account, e.g., temperature.
4. semaGIBAC does not require an accurate general forcefield for all atoms or a universal linear string/graph-based notation system, as it does not take 8Aib or C-18 fatty acid chain into account;

4. Conclusion

For the first time, this article puts forward a prototype GIBAC, i.e., semaGIBAC, to support the hypothesis that a real GIBAC is technically feasible in practice and of practical use for drug discovery and design:

1. semaGIBAC is able to calculate with 95.42% (27/28) accuracy the K_d between GLP-1R and any semaglutide analogue with one site-specific missense mutation introduced into its backbone.
2. semaGIBAC is able to be used the other way around as a search engine for drug design, i.e., for drug efficacy, semaGIBAC is able to generate a list of semaglutide analogue with one site-specific missense mutation introduced into its backbone, and rank them according to their average K_d (Table 4) values in the range of the minimum and the maximum values of semaGIBAC as included in Table 4, while for drug safety, semaGIBAC is unable to generate a K_d-ranked list of semaglutide analogues with suppressed off-target effects [78,79].
3. the construction of semaGIBAC consists of a set of in silico steps of structural and biophysical data generation towards a paradigm shift in precise drug discovery and design, leading to the identification of a promising semaglutide analogue with a K_d of 3.0×10^{-8} M, in contrast to the K_d of 3.278×10^{-6} M for native semaglutide and GLP-1R (PDB entry 4ZGM, Tables 2 and 4) [42].

5. Discussion

5.1. In Silico Generation of Structural and Biophysical Data with Reasonable Accuracy: Expanding Horizons in Precise Drug Discovery and Design

The past three years saw a big step forward in the use of artificial intelligence (AI) in structural biology for protein structure prediction [63,80–85], leading to the generation of computational structural data such as AlphaFold database [63,81–84]. Nonetheless, to train useful AI models for precise drug discovery and design, a huge number of data is needed with reasonable accuracy, buth experimental and synthetic, both structural and biophysical (K_d and ΔG), where a variety of tools are needed, such as molecular docking tools [86–89], molecular dynamics simulations tools [69,90], side chain placement and energy minimization algorithms [91] to incorporate structural arrangement information of post-translational modifications (PTMs) [92–94], post-expression modifications (PEMs) [6,74] into currently available structural models.

In this regard, this article puts forward a set of in silico steps of structural and biophysical data generation towards a paradigm shift in precise drug discovery and design [59,60]. Take semaglutide for instance, a five-dimensional semaGIBAC requires a total of 314496000000 (Table 5) homology structural models with 82.14% (23/28) homology to PDB ID: 4ZGM [42] to be built by Modeller [50], and subsequently a total of 314496000000 (Table 5) times of Prodigy-based [57,58] calculations of the binding affinities between semaglutide analogues and GLP-1R. Take MoleculeX (a protein consisting of 100 amino acids) as another example, the number soars from 314496000000 to 240920064000000 (Table 5).

 doi:10.20944/preprints202406.0953.v1

Table 5. The Size ($s = g(k,n) = \frac{k!}{n!(k-n)!} \times 20^n$) of the synthetic structural data set based on semaglutide-GLP-1R complex structure. where k represents the length of semaglutide backbone, n represents the number of missense mutations introduced into semaglutide backbone, where the value of n/k is key to ensure the overall reasonable accuracy of the synthetic structural data.

Size (s) of the synthetic structural and biophysical data set					
Semaglutide backbone (28 Aa)			**Molecule X (100 Aa)**		
g(28,1)	$\frac{28!}{1!(27)!} \times 20^1$	560	g(100,1)	$\frac{100!}{1!(99)!} \times 20^1$	2000
g(28,2)	$\frac{28!}{2!(26)!} \times 20^2$	151200	g(100,2)	$\frac{100!}{2!(98)!} \times 20^2$	1980000
g(28,3)	$\frac{28!}{3!(25)!} \times 20^3$	26208000	g(100,3)	$\frac{100!}{3!(97)!} \times 20^3$	1293600000
g(28,4)	$\frac{28!}{4!(24)!} \times 20^4$	3276000000	g(100,4)	$\frac{100!}{4!(96)!} \times 20^4$	627396000000
g(28,5)	$\frac{28!}{5!(23)!} \times 20^5$	314496000000	g(100,5)	$\frac{100!}{5!(95)!} \times 20^5$	240920064000000

In short, to build a real GIBAC using an entirely structural biophysics-based approach requires an exhaustive exploration of the entire molecular space (Figure 4) [61,77]. In practice, however, this astranomical task is computationally impossible, which explains partly why this article puts forward just only a structural biophysics-based prototype (i.e., semaGIBAC), instead of a real GIBAC. Therefore, this article here again proposes an AI-based **open** strategy [95] to make it possible and conceivable to generate a vast amount of data to train a real GIBAC with reasonable accuracy and precision, as openness in data acquisition and generation, and AI algorithms is essential for promoting transparency, reproducibility, and collaboration within the community of drug discovery & design, and for facilitating continued improvement of the performance (accuracy, precision and efficiency) of GIBAC in precise drug discovery & design [35,36] in future.

 doi:10.20944/preprints202406.0953.v1

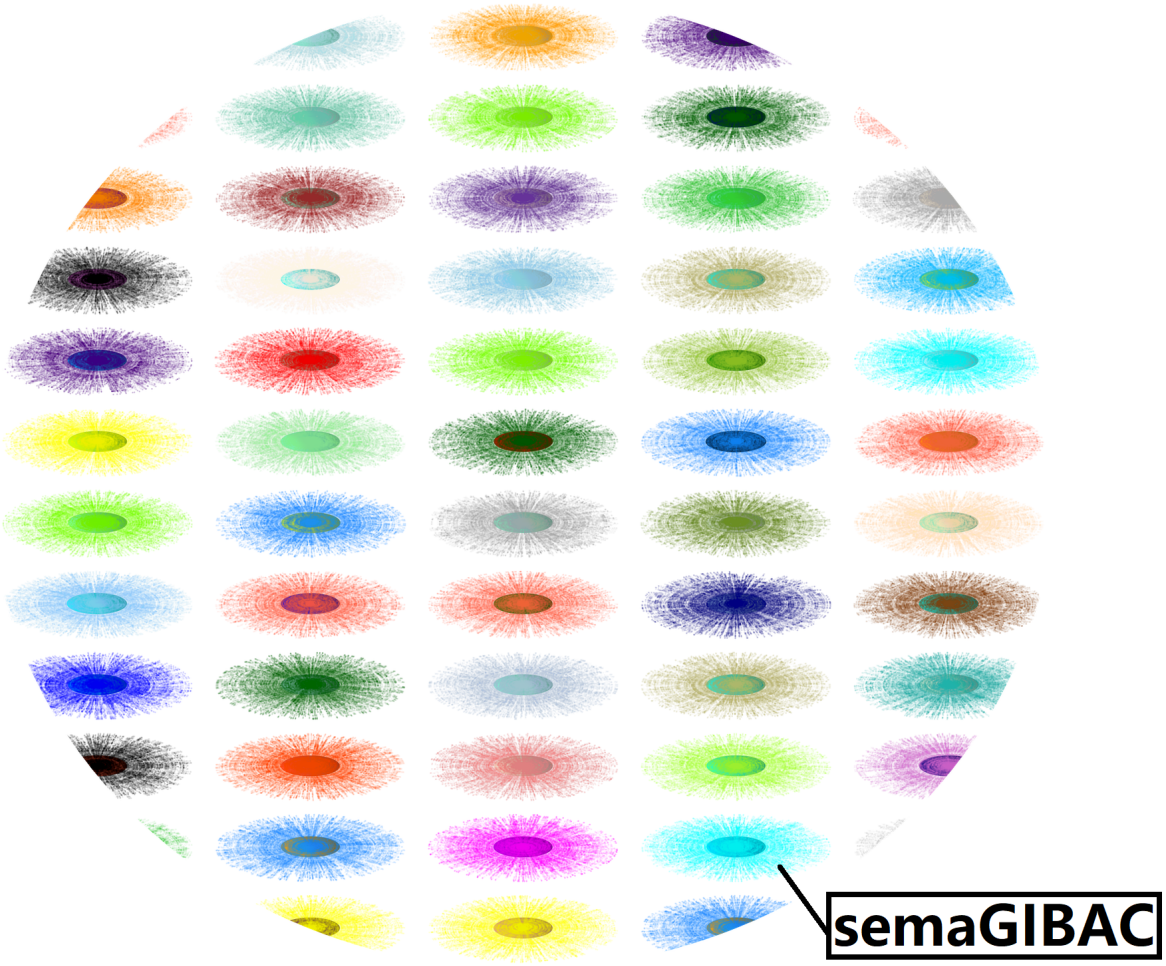

Figure 4. A partial sketch of the molecular space. In this figure, suppose the molecular space is an ocean with a series of islands, semaGIBAC is one of the island (hydrogen atom), consisting of experimental (nucleus) and computational (electron cloud) structural and biophysical data for any type of (bio)molecule within PDB.

As mentioned above, this article puts forward a set of in silico steps of structural and biophysical data generation towards a paradigm shift in precise drug discovery and design [59,60]. Specifically, here, the generation of synthetic structural and K_d data is akin to the distribution of the electron cloud of a hydrogen atom (Figure 4), where *Radius* is the distance between the electron (synthetic data) and the proton (i.e., nucleus, experimental data) of the hydrogen atom. With respect to semaGIBAC, PDB entry 4ZGM (Table 2) is the nucleus, while **Table S1** of supplementary file semaGIBAC.pdf is one layer of the electron cloud (Figure 4), while semaGIBAC itself is depicted in Figure 4 as one hydrogen atom. In principle, any biomolecule inside Protein Data Bank [37,39], i.e., experimental structural data, is able to be used as a hydrogen nucleus (Figure 4), around which there is an electron cloud representing a vast set of synthetic structural and biophysical data, while the white region of Figure 4 represents structurally and biophysically uncharted territories, highlighting an astranomical task which is computationally impossible, and calling for an AI-based **open** approach for the construction of a real GIBAC [35,36].

5.2. Designing Semaglutide Analogues with Elevated Binding Affinity and Efficacy through Continued Exploration of the Uncharted Molecular Space of Semaglutide and GLP-1R

The development of semaglutide analogues with increased GLP-1R binding affinity holds significant clinical relevance, offering the potential for enhanced glucose control, weight loss, and

 doi:10.20944/preprints202406.0953.v1

cardiovascular benefits in patients with type 2 diabetes and obesity [42,96,97]. Thanks to the continued development of experimental structural biology and the half-a-century old Protein Data Bank (PDB) [37–40,98], a comprehensive structural biophysical analysis becomes possible [99,100] for specific ligand-receptor complex structures deposited in PDB, such that our understanding of the structural and biophysical basis of their interfacial stability is able to help us modify the binding affinity of certain drug target and its interacting partners [101–103].

With semaglutide as an example here [59], one particular analogue (supplementary file **semx.pdb**, Table 6) stood out with four missense mutations (G13B_A, I20B_Q, L23B_R and V24B_N) through computational structural modeling and biophysics-based rational design, with a Prodigy-calculated K_d as low as 3.0×10^{-8} M at 37 °C (Table 6), while the K_d is 3.278×10^{-6} M (Table 4) for the binding of native semaglutide's backbone to GLP-1 at 37 °C. Technically, the structural biophysics-based rational design of this semaglutide analogue (supplementary file **semx.pdb**) is a tiny part of the task of the construction of a four-dimensional semaGIBAC, which requires a total of 3276000000 (Table 5) homology structural models with 85.71% (24/28) homology to PDB ID: 4ZGM [42] to be built by Modeller [50], and subsequently a total of 3276000000 (Table 5) times of Prodigy-based [57,58] calculations of the binding affinities between semaglutide analogues and GLP-1R. Given the size of the computational task, this article only puts forward one-dimensional semaGIBAC as a GIBAC prototype, making this semaglutide analogue (supplementary file **semx.pdb** look like a tip of the iceberg floating on the ocean (Figure 4) of a four-dimensional sequence space of semaglutide and GLP-1R (PDB entry 4ZGM [42], Table 2).

Table 6. The binding affinities of native semaglutide (4ZGM), semaglutide with a Val27-Arg28 exchange and semaglutideX (supplementary file **semx.pdb**, Table 6) to GLP-1R as calculated by Prodigy.

PDB file	Protein-Protein Complex	Δ G (kcal/mol)	Kd (M) at 37 °C	Fold
4ZGM [42]	semaglutide-GLP-1R [42]	-7.8	3.4×10^{-6}	1
sema.pdb [6]	Val27-Arg28 exchange [6]	-8.4	1.1×10^{-6}	3.09
semx.pdb [59]	G13B_A I20B_Q L23B_R V24B_N [59]	-10.7	3.0×10^{-8}	113.33

Of further note, the K_d of this semaglutide analogue (supplementary file **semx.pdb** is only a result of the structural biophysics-based calculation of Prodigy [57,58]. As a result, its real K_d and efficacy (in both vitro and vivo) need to be experimentally tested in wet-labs (Figure 5), as part of the drug discovery and design process in the early stage of drug R&D, which to date is still a lengthy, costly, difficult and inefficient yet pivotal process [104]. Given this, this article calls again for the construction of a real GIBAC [35,36] with adequate accuracy, precision and efficiency towards a paradigm shift [105] of precise drug discovery & design, until a real GIBAC comes into being and pushing forward the continued development of the industry [106–108].

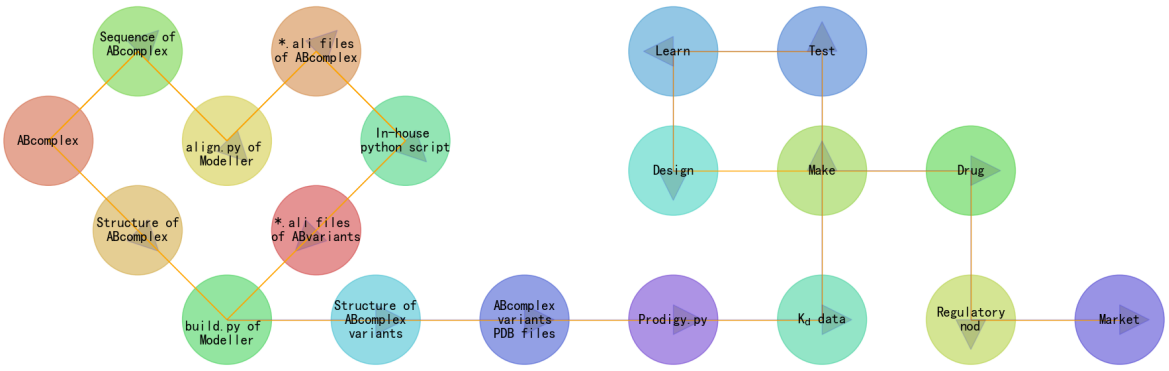

Figure 5. A future direction of in silico generation of structural and intermolecular K_d data in precise drug discovery & design. This figure is an extention of Figure 2

 doi:10.20944/preprints202406.0953.v1

6. Ethical Statement

No ethical approval is required.

7. Declaration of Generative AI and AI-Assisted Technologies in the Writing Process

During the preparation of this work, the author used OpenAI's ChatGPT in order to improve the readability of the manuscript, and to make it as concise and short as possible. After using this tool, the author reviewed and edited the content as needed and takes full responsibility for the content of the publication.

Author Contributions: Conceptualization, W.L.; methodology, W.L.; software, W.L.; validation, W.L.; formal analysis, W.L.; investigation, W.L.; resources, W.L.; data duration, W.L.; writing–original draft preparation, W.L.; writing–review and editing, W.L.; visualization, W.L.; supervision, W.L.; project administration, W.L.; funding acquisition, not applicable.

Funding: This research received no external funding.

Conflicts of Interest: The author declares no conflict of interest.

References

1. Murphy, K.M.; Gould, R.J.; Largent, B.L.; Snyder, S.H. A unitary mechanism of calcium antagonist drug action. *Proceedings of the National Academy of Sciences* **1983**, *80*, 860–864.
2. Zhang, Z.; Palzkill, T. Determinants of binding affinity and specificity for the interaction of TEM-1 and SME-1 β-lactamase with β-lactamase inhibitory protein. *J. Biol. Chem.* **2003**, *278*, 45706–45712.
3. Zhang, X.; Gao, H.; Wang, H.; Chen, Z.; Zhang, Z.; Chen, X.; Li, Y.; Qi, Y.; Wang, R. PLANET: A Multi-objective Graph Neural Network Model for Protein-Ligand Binding Affinity Prediction. *Journal of Chemical Information and Modeling* **2023**.
4. Li, W. High-Throughput Extraction of Interfacial Electrostatic Features from GLP-1-GLP-1R Complex Structures: A GLP-1-GLP-1R-Based Mini GIBAC Perspective **2024**. doi:10.20944/preprints202402.1519.v1.
5. Trosset, J.Y.; Cavé, C. In Silico Drug-Target Profiling. In *Target Identification and Validation in Drug Discovery*; Springer New York, 2019; pp. 89–103.
6. Li, W. Strengthening Semaglutide-GLP-1R Binding Affinity via a Val27-Arg28 Exchange in the Peptide Backbone of Semaglutide: A Computational Structural Approach. *Journal of Computational Biophysics and Chemistry* **2021**, *20*, 495–499.
7. Noble, D.; Blundell, T.L.; Kohl, P. Progress in biophysics and molecular biology: A brief history of the journal. *Progress in Biophysics and Molecular Biology* **2018**, *140*, 1–4.
8. Tsien, R.W.; Hess, P.; McCleskey, E.W.; Rosenberg, R.L. Calcium channels: Mechanisms of Selectivity, Permeation, and Block. *Annual Review of Biophysics and Biophysical Chemistry* **1987**, *16*, 265–290.
9. Greenidge, P.A.; Kramer, C.; Mozziconacci, J.C.; Wolf, R.M. MM/GBSA Binding Energy Prediction on the PDBbind Data Set: Successes, Failures, and Directions for Further Improvement. *Journal of Chemical Information and Modeling* **2012**, *53*, 201–209.
10. Su, M.; Yang, Q.; Du, Y.; Feng, G.; Liu, Z.; Li, Y.; Wang, R. Comparative Assessment of Scoring Functions: The CASF-2016 Update. *Journal of Chemical Information and Modeling* **2018**, *59*, 895–913.
11. Freire, E. Biophysical methods for the determination of protein-ligand binding constants. *Annual review of biophysics* **2009**, *38*, 123–142.
12. Johnson, C.M. Isothermal Calorimetry. In *Protein-Ligand Interactions*; Springer US, 2021; pp. 135–159.
13. Velázquez-Coy, A.; Ohtaka, H.; Nezami, A.; Muzammil, S.; Freire, E. Isothermal Titration Calorimetry. *Current Protocols in Cell Biology* **2004**, *23*.
14. Sauer, U.G. Surface plasmon resonance-a label-free tool for cellular analysis. *Journal of biotechnology* **2008**, *133*, 101–108.
15. Ernst, R.R.; Bodenhausen, G.; Wokaun, A. Principles of nuclear magnetic resonance in one and two dimensions. *Principles of nuclear magnetic resonance in one and two dimensions* **1990**, *14*.
16. Fuji, H.; Qi, F.; Qu, L.; Takaesu, Y.; Hoshino, T. Prediction of Ligand Binding Affinity to Target Proteins by Molecular Mechanics Theoretical Calculation. *Chemical and Pharmaceutical Bulletin* **2017**, *65*, 461–468.

 doi:10.20944/preprints202406.0953.v1

17. Gilson, M.K.; Zhou, H.X. Calculation of Protein-Ligand Binding Affinities. *Annual Review of Biophysics and Biomolecular Structure* **2007**, *36*, 21–42.
18. Li, W. Designing rt-PA Analogs to Release its Trapped Thrombolytic Activity. *Journal of Computational Biophysics and Chemistry* **2021**, *20*, 719–727.
19. Jubb, H.C.; Pandurangan, A.P.; Turner, M.A.; Ochoa-Montaño, B.; Blundell, T.L.; Ascher, D.B. Mutations at protein-protein interfaces: Small changes over big surfaces have large impacts on human health. *Progress in Biophysics and Molecular Biology* **2017**, *128*, 3–13.
20. Kulkarni-Kale, U.; Raskar-Renuse, S.; Natekar-Kalantre, G.; Saxena, S.A. Antigen-Antibody Interaction Database AgAbDb: A Compendium of Antigen-Antibody Interactions. In *Methods in Molecular Biology*; Springer New York, 2014; pp. 149–164.
21. Manso, T.; Folch, G.; Giudicelli, V.; Jabado-Michaloud, J.; Kushwaha, A.; Ngoune, V.N.; Georga, M.; Papadaki, A.; Debbagh, C.; Pégorier, P.; Bertignac, M.; Hadi-Saljoqi, S.; Chentli, I.; Cherouali, K.; Aouinti, S.; Hamwi, A.E.; Albani, A.; Elhassani, M.E.; Viart, B.; Goret, A.; Tran, A.; Sanou, G.; Rollin, M.; Duroux, P.; Kossida, S. IMGT® databases, related tools and web resources through three main axes of research and development. *Nucleic Acids Research* **2021**, *50*, D1262–D1272.
22. Xu, D.; Zhang, Y. Improving the physical realism and structural accuracy of protein models by a two-step atomic-level energy minimization. *Biophys. J.* **2011**, *101*, 2525–2534.
23. Li, W.; Shi, G. How $Ca_V1.2$-bound verapamil blocks Ca^{2+} influx into cardiomyocyte: Atomic level views. *Pharmacological Research* **2019**, *139*, 153–157.
24. Li, W. Delving deep into the structural aspects of a furin cleavage site inserted into the spike protein of SARS-CoV-2: A structural biophysical perspective. *Biophysical Chemistry* **2020**, *264*, 106420.
25. Pieber, T.R.; Bode, B.; Mertens, A.; Cho, Y.M.; Christiansen, E.; Hertz, C.L.; Wallenstein, S.O.R.; Buse, J.B.; Akın, S.; Aladağ, N.; Arif, A.A.; Aronne, L.J.; Aronoff, S.; Ataoglu, E.; Baik, S.H.; Bays, H.; Beckett, P.L.; Berker, D.; Bilz, S.; Bode, B.; Braun, E.W.; Buse, J.B.; Canani, L.H.S.; Cho, Y.M.; Chung, C.H.; Colin, I.; Condit, J.; Cooper, J.; Delgado, B.; Eagerton, D.C.; Ebrashy, I.N.E.; Hefnawy, M.H.M.F.E.; Eliaschewitz, F.G.; Finneran, M.P.; Fischli, S.; Fließer-Görzer, E.; Geohas, J.; Godbole, N.A.; Golay, A.; de Lapertosa, S.G.; Gross, J.L.; Gulseth, H.L.; Helland, F.; Høivik, H.O.; Issa, C.; Kang, E.S.; Keller, C.; Khalil, S.H.A.; Kim, N.H.; Kim, I.J.; Klaff, L.J.; Laimer, M.; LaRocque, J.C.; Lederman, S.N.; Lee, K.W.; Litchfield, W.R.; Manning, M.B.; Mertens, A.; Morawski, E.J.; Murray, A.V.; Nicol, P.R.; O'Connor, T.M.; Oğuz, A.; Ong, S.; özdemir, A.; Palace, E.M.; Palchick, B.A.; Pereles-Ortiz, J.; Pieber, T.; Prager, R.; Preumont, V.; Riffer, E.; Rista, L.; Rudofsky, G.; Sarı, R.; Scheen, A.; Schultes, B.; Seo, J.A.; Shelbaya, S.A.; Sivalingam, K.; Sorli, C.H.; Stäuble, S.; Streja, D.A.; T'Sjoen, G.; Tetiker, T.; Gaal, L.V.; Vercammen, C.; Warren, M.L.; Weinstein, D.L.; Weiss, D.; White, A.; Winnie, M.; Wium, C.; Yavuz, D. Efficacy and safety of oral semaglutide with flexible dose adjustment versus sitagliptin in type 2 diabetes (PIONEER 7): a multicentre, open-label, randomised, phase 3a trial. *The Lancet Diabetes & Endocrinology* **2019**, *7*, 528–539.
26. Lingvay, I.; Catarig, A.M.; Frias, J.P.; Kumar, H.; Lausvig, N.L.; le Roux, C.W.; Thielke, D.; Viljoen, A.; McCrimmon, R.J. Efficacy and safety of once-weekly semaglutide versus daily canagliflozin as add-on to metformin in patients with type 2 diabetes (SUSTAIN 8): a double-blind, phase 3b, randomised controlled trial. *The Lancet Diabetes & Endocrinology* **2019**, *7*, 834–844.
27. Li, Y.; Su, M.; Liu, Z.; Li, J.; Liu, J.; Han, L.; Wang, R. Assessing protein-ligand interaction scoring functions with the CASF-2013 benchmark. *Nature Protocols* **2018**, *13*, 666–680.
28. Law, V.; Knox, C.; Djoumbou, Y.; Jewison, T.; Guo, A.C.; Liu, Y.; Maciejewski, A.; Arndt, D.; Wilson, M.; Neveu, V.; Tang, A.; Gabriel, G.; Ly, C.; Adamjee, S.; Dame, Z.T.; Han, B.; Zhou, Y.; Wishart, D.S. DrugBank 4.0: shedding new light on drug metabolism. *Nucleic Acids Research* **2013**, *42*, D1091–D1097.
29. Li, W. Designing Insulin Analogues with Lower Binding Affinity to Insulin Receptor than That of Insulin Icodec **2024**. doi:10.20944/preprints202404.1922.v1.
30. Li, W. A GIBAC-based selectivity strategy for the design of PDE5 inhibitors to minimize visual disturbances **2024**. doi:10.20944/preprints202405.1374.v1.
31. Bischoff, E. Potency, selectivity, and consequences of nonselectivity of PDE inhibition. *International Journal of Impotence Research* **2004**, *16*, S11–S14. doi:10.1038/sj.ijir.3901208.
32. Ahmed, S.; Atia, N.N.; Rageh, A.H. Selectivity enhanced cation exchange chromatography for simultaneous determination of peptide variants. *Talanta* **2019**, *199*, 347–354.

33. Tinberg, C.E.; Khare, S.D.; Dou, J.; Doyle, L.; Nelson, J.W.; Schena, A.; Jankowski, W.; Kalodimos, C.G.; Johnsson, K.; Stoddard, B.L.; Baker, D. Computational design of ligand-binding proteins with high affinity and selectivity. *Nature* **2013**, *501*, 212–216.
34. Almers, W.; McCleskey, E.W. Non-selective conductance in calcium channels of frog muscle: calcium selectivity in a single-file pore. *The Journal of Physiology* **1984**, *353*, 585–608.
35. Li, W. Towards a General Intermolecular Binding Affinity Calculator **2022**.
36. Li, W.; Vottevor, G. Towards a Truly General Intermolecular Binding Affinity Calculator for Drug Discovery & Design **2023**.
37. Berman, H.; Henrick, K.; Nakamura, H. Announcing the worldwide Protein Data Bank. *Nature Structural & Molecular Biology* **2003**, *10*, 980–980.
38. Li, W. Half-a-century Burial of ρ, θ, and φ in PDB **2021**.
39. Li, W. Visualising the Experimentally Uncharted Territories of Membrane Protein Structures inside Protein Data Bank **2020**.
40. Li, W. A Local Spherical Coordinate System Approach to Protein 3D Structure Description **2020**.
41. Li, W. A Reversible Spherical Geometric Conversion of Protein Backbone Structure Coordinate Matrix to Three Independent Vectors of ρ, ϑ and φ **2024**. doi:10.20944/preprints202404.0576.v1.
42. Lau, J.; Bloch, P.; Schäffer, L.; Pettersson, I.; Spetzler, J.; Kofoed, J.; Madsen, K.; Knudsen, L.B.; McGuire, J.; Steensgaard, D.B.; Strauss, H.M.; Gram, D.X.; Knudsen, S.M.; Nielsen, F.S.; Thygesen, P.; Reedtz-Runge, S.; Kruse, T. Discovery of the Once-Weekly Glucagon-Like Peptide-1 (GLP-1) Analogue Semaglutide. *Journal of Medicinal Chemistry* **2015**, *58*, 7370–7380.
43. Rodbard, H.W.; Rosenstock, J.; Canani, L.H.; Deerochanawong, C.; Gumprecht, J.; Lindberg, S.Ø.; Lingvay, I.; Søndergaard, A.L.; Treppendahl, M.B.; Montanya, E. Oral Semaglutide Versus Empagliflozin in Patients With Type 2 Diabetes Uncontrolled on Metformin: The PIONEER 2 Trial. *Diabetes Care* **2019**, *42*, 2272–2281.
44. Pratley, R.; Amod, A.; Hoff, S.T.; Kadowaki, T.; Lingvay, I.; Nauck, M.; Pedersen, K.B.; Saugstrup, T.; Meier, J.J. Oral semaglutide versus subcutaneous liraglutide and placebo in type 2 diabetes (PIONEER 4): a randomised, double-blind, phase 3a trial. *The Lancet* **2019**, *394*, 39–50.
45. Røder, M.E. Clinical potential of treatment with semaglutide in type 2 diabetes patients. *Drugs in Context* **2019**, *8*, 1–11.
46. Hofmann, D.W.M.; Kuleshova, L.N. A general force field by machine learning on experimental crystal structures. Calculations of intermolecular Gibbs energy with iFlexCryst. *Acta Crystallographica Section A Foundations and Advances* **2023**, *79*, 132–144.
47. Giannakoulias, S.; Shringari, S.R.; Ferrie, J.J.; Petersson, E.J. Biomolecular simulation based machine learning models accurately predict sites of tolerability to the unnatural amino acid acridonylalanine. *Scientific Reports* **2021**, *11*. doi:10.1038/s41598-021-97965-2.
48. Zhang, H.; Zheng, Z.; Dong, L.; Shi, N.; Yang, Y.; Chen, H.; Shen, Y.; Xia, Q. Rational incorporation of any unnatural amino acid into proteins by machine learning on existing experimental proofs. *Computational and Structural Biotechnology Journal* **2022**, *20*, 4930–4941. doi:10.1016/j.csbj.2022.08.063.
49. Li, W. How Structural Modifications of Insulin Icodec Contributes to Its Prolonged Duration of Action: A Structural and Biophysical Perspective **2023**. doi:10.20944/preprints202311.1048.v1.
50. Webb, B.; Sali, A. Protein Structure Modeling with MODELLER. In *Methods in Molecular Biology*; Springer US, 2020; pp. 239–255.
51. Li, W. Gravity-driven pH adjustment for site-specific protein pK_a measurement by solution-state NMR. *Measurement Science and Technology* **2017**, *28*, 127002.
52. Webb, H.; Tynan-Connolly, B.M.; Lee, G.M.; Farrell, D.; O'Meara, F.; Søndergaard, C.R.; Teilum, K.; Hewage, C.; McIntosh, L.P.; Nielsen, J.E. Remeasuring HEWL pKa values by NMR spectroscopy: Methods, analysis, accuracy, and implications for theoretical pKa calculations. *Proteins: Structure, Function, and Bioinformatics* **2010**, *79*, 685–702.
53. Hansen, A.L.; Kay, L.E. Measurement of histidine pK_a values and tautomer populations in invisible protein states. *Proceedings of the National Academy of Sciences* **2014**, *111*.
54. Olsson, M.H.M.; Søndergaard, C.R.; Rostkowski, M.; Jensen, J.H. PROPKA3: Consistent Treatment of Internal and Surface Residues in Empirical pK_a Predictions. *Journal of Chemical Theory and Computation* **2011**, *7*, 525–537.

55. Ahrén, B.; Atkin, S.L.; Charpentier, G.; Warren, M.L.; Wilding, J.P.H.; Birch, S.; Holst, A.G.; Leiter, L.A. Semaglutide induces weight loss in subjects with type 2 diabetes regardless of baseline BMI or gastrointestinal adverse events in the SUSTAIN 1 to 5 trials. *Diabetes, Obesity and Metabolism* **2018**, *20*, 2210–2219.
56. Aroda, V.R.; Rosenstock, J.; Terauchi, Y.; Altuntas, Y.; Lalic, N.M.; Villegas, E.C.M.; Jeppesen, O.K.; Christiansen, E.; Hertz, C.L.; Haluzík, M. PIONEER 1: Randomized Clinical Trial of the Efficacy and Safety of Oral Semaglutide Monotherapy in Comparison With Placebo in Patients With Type 2 Diabetes. *Diabetes Care* **2019**, *42*, 1724–1732.
57. Vangone, A.; Bonvin, A.M. Contacts-based prediction of binding affinity in protein–protein complexes. *eLife* **2015**, *4*.
58. Xue, L.C.; Rodrigues, J.P.; Kastritis, P.L.; Bonvin, A.M.; Vangone, A. PRODIGY: a web server for predicting the binding affinity of protein–protein complexes. *Bioinformatics* **2016**, p. btw514.
59. Li, W. An Exhaustive Exploration of the Semaglutide-GLP-1R Sequence Space towards the Design of Semaglutide Analogues with Elevated Binding Affinity to GLP-1R **2024**. doi:10.20944/preprints202405.0258.v1.
60. Li, W. In Silico Generation of Structural and Intermolecular Binding Affinity Data with Reasonable Accuracy: Expanding Horizons in Drug Discovery and Design **2024**. doi:10.20944/preprints202405.1739.v1.
61. Wang, T.; He, X.; Li, M.; Shao, B.; Liu, T.Y. AIMD-Chig: Exploring the conformational space of a 166-atom protein Chignolin with ab initio molecular dynamics. *Scientific Data* **2023**, *10*.
62. Shulman, R.; Wüthrich, K.; Yamane, T.; Patel, D.J.; Blumberg, W. Nuclear magnetic resonance determination of ligand-induced conformational changes in myoglobin. *Journal of Molecular Biology* **1970**, *53*, 143–157.
63. Tong, A.B.; Burch, J.D.; McKay, D.; Bustamante, C.; Crackower, M.A.; Wu, H. Could AlphaFold revolutionize chemical therapeutics? *Nature Structural & Molecular Biology* **2021**, *28*, 771–772.
64. Ruff, K.M.; Pappu, R.V. AlphaFold and Implications for Intrinsically Disordered Proteins. *Journal of Molecular Biology* **2021**, p. 167208.
65. Higgins, M.K. Can We AlphaFold Our Way Out of the Next Pandemic? *Journal of Molecular Biology* **2021**, p. 167093.
66. Platzer, G.; Okon, M.; McIntosh, L.P. pH-dependent random coil 1H, 13C, and 15N chemical shifts of the ionizable amino acids: a guide for protein pK_a measurements. *Journal of Biomolecular NMR* **2014**, *60*, 109–129.
67. Yang, A.S.; Honig, B. On the pH Dependence of Protein Stability. *Journal of Molecular Biology* **1993**, *231*, 459–474.
68. Harris, T.K.; Turner, G.J. Structural Basis of Perturbed pK_a Values of Catalytic Groups in Enzyme Active Sites. *IUBMB Life (International Union of Biochemistry and Molecular Biology: Life)* **2002**, *53*, 85–98.
69. Li, W. Characterising the interaction between caenopore-5 and model membranes by NMR spectroscopy and molecular dynamics simulations. PhD thesis, University of Auckland, 2016.
70. Hansen, A.L.; Kay, L.E. Measurement of histidine pK_a values and tautomer populations in invisible protein states. *Proceedings of the National Academy of Sciences* **2014**, *111*, E1705–E1712.
71. Box, K.; Bevan, C.; Comer, J.; Hill, A.; Allen, R.; Reynolds, D. High-Throughput Measurement of pKa Values in a Mixed-Buffer Linear pH Gradient System. *Analytical Chemistry* **2003**, *75*, 883–892.
72. Petukh, M.; Stefl, S.; Alexov, E. The Role of Protonation States in Ligand-Receptor Recognition and Binding. *Current Pharmaceutical Design* **2013**, *19*, 4182–4190.
73. Søndergaard, C.R.; Olsson, M.H.M.; Rostkowski, M.; Jensen, J.H. Improved Treatment of Ligands and Coupling Effects in Empirical Calculation and Rationalization of pK_a Values. *Journal of Chemical Theory and Computation* **2011**, *7*, 2284–2295.
74. Weiss, M. Design of ultra-stable insulin analogues for the developing world. *Journal of Health Specialties* **2013**, *1*, 59.
75. Nuhoho, S.; Gupta, J.; Hansen, B.B.; Fletcher-Louis, M.; Dang-Tan, T.; Paine, A. Orally Administered Semaglutide Versus GLP-1 RAs in Patients with Type 2 Diabetes Previously Receiving 1–2 Oral Antidiabetics: Systematic Review and Network Meta-Analysis. *Diabetes Therapy* **2019**, *10*, 2183–2199.
76. Bucheit, J.D.; Pamulapati, L.G.; Carter, N.; Malloy, K.; Dixon, D.L.; Sisson, E.M. Oral Semaglutide: A Review of the First Oral Glucagon-Like Peptide 1 Receptor Agonist. *Diabetes Technology & Therapeutics* **2020**, *22*, 10–18.

77. Müller, C.E.; Hansen, F.K.; Gütschow, M.; Lindsley, C.W.; Liotta, D. New Drug Modalities in Medicinal Chemistry, Pharmacology, and Translational Science. *ACS Pharmacology & Translational Science* **2021**, *4*, 1712–1713.
78. He, Y.; Su, J.; Lan, B.; Gao, Y.; Zhao, J. Targeting off-target effects: endoplasmic reticulum stress and autophagy as effective strategies to enhance temozolomide treatment. *OncoTargets and Therapy* **2019**, *Volume 12*, 1857–1865. doi:10.2147/ott.s194770.
79. Tsai, S.Q.; Nguyen, N.T.; Malagon-Lopez, J.; Topkar, V.V.; Aryee, M.J.; Joung, J.K. CIRCLE-seq: a highly sensitive in vitro screen for genome-wide CRISPR-Cas9 nuclease off-targets. *Nature Methods* **2017**, *14*, 607–614.
80. Wang, Y.; Wang, L.; Shen, Y.; Wang, Y.; Yuan, H.; Wu, Y.; Gu, Q. Protein Conformation Generation via Force-Guided SE(3) Diffusion Models, 2024. doi:10.48550/ARXIV.2403.14088.
81. Callaway, E. The entire protein universe: AI predicts shape of nearly every known protein. *Nature* **2022**.
82. Waterhouse, A.; Bertoni, M.; Bienert, S.; Studer, G.; Tauriello, G.; Gumienny, R.; Heer, F.T.; de Beer, T.A.P.; Rempfer, C.; Bordoli, L.; Lepore, R.; Schwede, T. SWISS-MODEL: homology modelling of protein structures and complexes. *Nucleic Acids Research* **2018**, *46*, W296–W303.
83. Hasani, H.J.; Barakat, K. Homology Modeling: an Overview of Fundamentals and Tools. *International Review on Modelling and Simulations (IREMOS)* **2017**, *10*, 129.
84. Pettersen, E.F.; Goddard, T.D.; Huang, C.C.; Couch, G.S.; Greenblatt, D.M.; Meng, E.C.; Ferrin, T.E. UCSF Chimera: A visualization system for exploratory research and analysis. *Journal of Computational Chemistry* **2004**, *25*, 1605–1612.
85. Gircha, A.I.; Boev, A.S.; Avchaciov, K.; Fedichev, P.O.; Fedorov, A.K. Hybrid quantum-classical machine learning for generative chemistry and drug design. *Scientific Reports* **2023**, *13*. doi:10.1038/s41598-023-32703-4.
86. Roggia, M.; Natale, B.; Amendola, G.; Maro, S.D.; Cosconati, S. Streamlining Large Chemical Library Docking with Artificial Intelligence: the PyRMD2Dock Approach. *Journal of Chemical Information and Modeling* **2023**.
87. Agu, P.C.; Afiukwa, C.A.; Orji, O.U.; Ezeh, E.M.; Ofoke, I.H.; Ogbu, C.O.; Ugwuja, E.I.; Aja, P.M. Molecular docking as a tool for the discovery of molecular targets of nutraceuticals in diseases management. *Scientific Reports* **2023**, *13*.
88. Zheng, Z.; Merz, K.M. Calculating protein-ligand binding affinities with MMPBSA: Method and error analysis. *Journal of chemical theory and computation* **2017**, *13*, 4751–4767.
89. Deng, N.J.; Zheng, Q.; Liu, J.; Hao, G.F. Predicting protein–ligand binding affinity with a random matrix framework. *PLoS computational biology* **2012**, *8*, e1002775.
90. Karplus, M.; McCammon, J.A. Molecular dynamics simulations of biomolecules. *Nature structural biology* **2002**, *9*, 646–652.
91. Canzar, S.; Toussaint, N.C.; Klau, G.W. An exact algorithm for side-chain placement in protein design. *Optimization Letters* **2011**, *5*, 393–406.
92. Herget, S.; Ranzinger, R.; Maass, K.; Lieth, C.W. GlycoCT—a unifying sequence format for carbohydrates. *Carbohydrate Research* **2008**, *343*, 2162–2171.
93. Foster, J.M.; Moreno, P.; Fabregat, A.; Hermjakob, H.; Steinbeck, C.; Apweiler, R.; Wakelam, M.J.O.; Vizcaíno, J.A. LipidHome: A Database of Theoretical Lipids Optimized for High Throughput Mass Spectrometry Lipidomics. *PLoS ONE* **2013**, *8*, e61951.
94. Sud, M.; Fahy, E.; Subramaniam, S. Template-based combinatorial enumeration of virtual compound libraries for lipids. *Journal of Cheminformatics* **2012**, *4*.
95. Hanson, B.; Stall, S.; Cutcher-Gershenfeld, J.; Vrouwenvelder, K.; Wirz, C.; Rao, Y.; Peng, G. Garbage in, garbage out: mitigating risks and maximizing benefits of AI in research. *Nature* **2023**, *623*, 28–31.
96. Blüher, M.; Rosenstock, J.; Hoefler, J.; Manuel, R.; Hennige, A.M. Dose–response effects on HbA1c and bodyweight reduction of survodutide, a dual glucagon/GLP-1 receptor agonist, compared with placebo and open-label semaglutide in people with type 2 diabetes: a randomised clinical trial. *Diabetologia* **2023**, *67*, 470–482. doi:10.1007/s00125-023-06053-9.
97. Knudsen, L.B.; Lau, J. The Discovery and Development of Liraglutide and Semaglutide. *Frontiers in Endocrinology* **2019**, *10*, 1–32.
98. Li, W. Structurally Observed Electrostatic Features of the COVID-19 Coronavirus-Related Experimental Structures inside Protein Data Bank: A Brief Update **2020**.

99. Li, W. How do SMA-linked mutations of *SMN1* lead to structural/functional deficiency of the SMA protein? *PLOS ONE* **2017**, *12*, e0178519.
100. Li, W. Extracting the Interfacial Electrostatic Features from Experimentally Determined Antigen and/or Antibody-Related Structures inside Protein Data Bank for Machine Learning-Based Antibody Design **2020**.
101. Li, W. Calcium Channel Trafficking Blocker Gabapentin Bound to the α-2-δ-1 Subunit of Voltage-Gated Calcium Channel: A Computational Structural Investigation **2020**.
102. Li, W. Inter-Molecular Electrostatic Interactions Stabilizing the Structure of the PD-1/PD-L1 Axis: A Structural Evolutionary Perspective **2020**.
103. Li, W. Designing Nerve Growth Factor Analogues to Suppress Pain Signal Transduction Mediated by the p75NTR-NGF-TrkA Complex: A Structural and Biophysical Perspective **2024**. doi:10.20944/preprints202403.1756.v1.
104. Zhou, S.F.; Zhong, W.Z. Drug Design and Discovery: Principles and Applications. *Molecules* **2017**, *22*, 279.
105. Subramaniam, S.; Kleywegt, G.J. A paradigm shift in structural biology. *Nature Methods* **2022**, *19*, 20–23.
106. Bonvin, A.M.J.J. 50 years of PDB: a catalyst in structural biology. *Nature Methods* **2021**, *18*, 448–449.
107. Vakili, M.G.; Gorgulla, C.; Nigam, A.; Bezrukov, D.; Varoli, D.; Aliper, A.; Polykovsky, D.; Das, K.M.P.; Snider, J.; Lyakisheva, A.; Mansob, A.H.; Yao, Z.; Bitar, L.; Radchenko, E.; Ding, X.; Liu, J.; Meng, F.; Ren, F.; Cao, Y.; Stagljar, I.; Aspuru-Guzik, A.; Zhavoronkov, A. Quantum Computing-Enhanced Algorithm Unveils Novel Inhibitors for KRAS, 2024. doi:10.48550/ARXIV.2402.08210.
108. Gupta, R.; Srivastava, D.; Sahu, M.; Tiwari, S.; Ambasta, R.K.; Kumar, P. Artificial intelligence to deep learning: machine intelligence approach for drug discovery. *Molecular Diversity* **2021**, *25*, 1315–1360.